Sensing and Bio-Sensing Research 28 (2020) 100333

Contents lists available at ScienceDirect

Sensing and Bio-Sensing Research

journal homepage: www.elsevier.com/locate/sbsr

Paper-based (bio)sensor for label-free detection of 3-nitrotyrosine in human urine samples using molecular imprinted polymer

Gabriela V. Martins[a,b,c,d], Ana C. Marques[a,b,c], Elvira Fortunato[c], M. Goreti F. Sales[a,b,d,*]

[a] BioMark/UC, Faculty of Science and Technology, Coimbra University, Portugal
[b] BioMark/ISEP, School of Engineering of the Polytechnique School, Porto, Portugal
[c] i3N/CENIMAT, Department of Materials Science, Faculty of Sciences and Technology, Universidade Nova de Lisboa and CEMOP/UNINOVA, Campus de Caparica, Portugal
[d] CEB – Centre of Biological Engineering, University of Minho, 4710-057 Braga, Portugal

ARTICLE INFO

Keywords:
3-nitrotyrosine
Molecular imprinted polymer
Electrochemical (bio)sensor
Urine biomarker
Carbon-printed electrode

ABSTRACT

Over the last years, paper technology has been widely spread as a more affordable, sustainable and reliable support material to be incorporated in the design of point-of-care (POC) diagnostic devices. However, the single work employing a paper-based device for 3-nitrotyrosine (3-NT), a relevant biomarker for oxidative stress (OS) that is a major origin for many diseases, is incapable of reading successfully complex samples because every species that oxidizes before ~0.75 V will also contribute to the final response. Thus, the introduction of a selective element was made into this set-up by including a molecularly-imprinted polymer (MIP) tailored in-situ.

Herein, a novel MIP for 3-NT was assembled directly on a paper platform, made conductive with carbon ink and suitable for an electrochemical transduction. The biomimetic material was produced by electropolymerization of phenol after optimizing several experimental parameters, such a scan-rate, number of cycles, range of potential applied, monomer and template concentrations. Under optimal conditions, the label-free sensor was able to respond to 3-NT from 500 nM to 1 mM, yielding a limit of detection of 22.3 nM. Finally, the applicability of the (bio)sensor was tested by performing calibration assays in human urine samples and a good performance was obtained in terms of sensitivity, selectivity and reproducibility.

Overall, the attributes of the herein described sensing approach can be compared to a very limited number of other electrochemical devices, that are still using a conventional three electrode system, making this paper-sustained device the first electrochemical (bio)sensor with potential to become a portable and low-cost diagnostic tool for 3-NT. In general, the incorporation of molecular imprinting technology coupled to electrochemical transduction enabled the fabrication of suitable smart sensors for wide screening approaches.

1. Introduction

In general, an electrochemical (bio)sensor constitutes an integrated device that provides analytical information, by using a bio-recognition element involved with an electrochemical transducer [1]. Additionally, screen-printed electrodes (SPEs) have been preferred against the conventional three-electrode system because these are disposable, easy-to-use and may operate with minimal volumes of analyte solutions. The basic steps in screen-printing microfabrication include the application of a suitable conductive ink on planar substrate materials, followed by a proper thermal cure [2,3]. Another great advantage of these electrodes is their ability to be drawn in different shapes and sizes, using different kinds of materials.

In recent years, paper has been chosen as the ideal support material to develop screen-printed (bio)sensor devices, due to its special characteristics, such as, flexibility, porosity, biocompatibility, facile modification, low-cost and sustainability [4,5]. The incorporation of this light and widely available natural resource has boosted the development of compact and miniaturized electrochemical devices, holding high sensitivity and selectivity [6]. A facile paper-based visual sensor for detecting anthrax molecule has been developed by using filter paper immobilized with Tb/DPA@SiO2-Eu/GMP, enabling direct observation of the colour switch from green to red by naked eyes under a UV lamp [7]. Moreover, a disposable paper-based platform with a bipolar electrochemical device was reported for the sensitive detection of the cancer marker prostate specific antigen (PSA), highlighting important

* Corresponding author at: Department of Chemical Engineering, Faculty of Science and Technology, University of Coimbra, Rua Sílvio Lima, Polo II, 3030-790 Coimbra, Portugal.
E-mail address: goreti.sales@eq.uc.pt (M.G.F. Sales).

https://doi.org/10.1016/j.sbsr.2020.100333
Received 29 December 2019; Received in revised form 25 February 2020; Accepted 28 February 2020

sensing features, such as simplicity, portability and disposability [8].

At this point, the combination of low-cost paper-based devices with SPE technology has greatly spread their application as simplified analytical systems in different areas, like, biomedical, environment and food monitoring. However, only very few studies have been able to fully integrate paper as a material-platform for the development of sensitive and selective electrochemical detection. As an example, fully-printed SPE was developed to target 3-nitrotyrosine (3-NT) directly, by means of its oxidation, with a maximum peak occurring at ~0.75 V [9]. Yet, this direct reading approach may lead to inaccurate data when complex samples are analysed, because every compound present that holds the ability to oxidize at lower potential shall contribute to a positive error.

To solve this drawback of direct electrochemical readings, the introduction of a discriminating element in the sensing area may be required. Overall, the incorporation of molecularly imprinted polymers (MIPs) in the architecture of (bio)sensors has been proven an efficient way to enhance the selectivity of the sensor device [10–13]. MIP technology tends to mimic the behaviour of antibodies, involving the formation of specific recognition sites, that fit in both shape and size. Among the different ways of MIP synthesis, electropolymerization enables the direct deposition of the sensing material on the transducer surface, allowing a facile and easy control of the film growth [14], which are suitable features for point-of-care (POC) analysis. During the electrosynthesis of MIPs, the compatibility of the functional monomer against the target-molecule is a crucial issue that also dictates the performance of the biosensing device [15,16].

The use of MIP materials to improve the analytical signal generated by paper-based SPEs was tested herein (for the first time in SPE-office paper based technology) by tailoring a molecularly MIP material for 3-NT on the working electrode area of the paper-based SPE. The MIP film for 3-NT was grown in-situ by electropolymerizing phenol. The selection of 3-NT for the purposes of this work accounts the fact that it is a biomarker of oxidative stress (OS), being ultimately related to chronic disease installation. Under OS, reactive oxygen species (ROS) or, also, reactive nitrogen species (RNS) are overproduced, yielding cellular damage in proteins, DNA and lipids [17,18]. In this context, 3-nitrotyrosine (3-NT) is a sub-product generated during protein attack by free radicals [19,20] and has been proposed as a relevant biomarker of OS [21]. For now, there is no consensus related to the basal levels of free 3-NT in human urine samples, but most reported methods have presented concentrations of few nM in healthy subjects [22]. There are some conventional methods to quantify 3-NT, including, liquid chromatography methods coupled with ultraviolet [23], fluorescence [24], mass spectrometry [25] and electrochemical detection [26], gas-chromatography-mass spectrometry [27] and immunoassays [28]. Although each one of these approaches holds unique advantages, mostly, high sensitivity and low limits of detection, these methods involve expensive apparatus and/or reagents, with complex procedure steps, being restricted to laboratorial use. There are also few reported sensors for the detection of 3-NT in biological matrices (Table 1), but these employ complex arrangements and signal amplification steps, such as, the incorporation of nanostructured materials, in order to obtain low detection limits. These technical approaches increase the cost of the overall sensing device and limit their disposability features, which are especially relevant if applied in wide screening approaches for early disease diagnostics. These methods also employ a reading probe, for which the development of a label-free method would be a beneficial feature in POC use.

Thus, this work combines (i) the advantages of having a paper substrate to design a low-cost and environmentally-friendly electrochemical sensing platform for the direct (and label-free) 3-NT detection; with the (ii) requirements of having a selective element within the sensing system, which is a molecular imprinting approach tailored in-situ, in order to develop a sensitive and selective label-free electrochemical (bio)sensor for assessing 3-NT. Herein, after careful optimization, the electropolymerization of phenol was performed by cyclic voltammetry (CV) over the potential range + 0.2 to +0.8 V in KCl (0.1 M) aqueous solution at 50 mV/s scan-rate and using 5 cycles. Moreover, our best electrochemical response for 3-NT was accomplished with a template-monomer ratio of 2:1.

2. Material and methods

2.1. Reagents

All reagents were of analytical grade and used without further purification. Buffer and electrolyte solutions were prepared with ultrapure water Mili-Q laboratory grade. The pH measurements were made in a pH meter from *Crison Instruments*, GLP21 model. Potassium hexacyanoferrate III ($K_3[Fe(CN)_6]$), potassium hexacyanoferrate II ($K_4[Fe(CN)_6]$) trihydrate and dipotassium hydrogen phosphate (K_2HPO_4) were obtained from Riedel-de-Haen; potassium dihydrogenophosphate (KH_2PO_4) was obtained from Panreac; potassium chloride (KCl) was from Merck; phenol (C_6H_5OH, for molecular biology) and sulphuric acid 95–97% (H_2SO_4) were from Sigma-Aldrich; phosphate buffered saline (PBS) tablets from Amresco and 3-nitro-L-tyrosine 98% (3-NT) from Alfa Aesar. Potassium phosphate buffer solutions (0.1 M, pH 6.0) and (0.2 M, pH 7.0) were prepared by mixing the proper amount of K_2HPO_4 and KH_2PO_4. All experiments were performed at ambient temperature.

2.2. Apparatus

The (bio)sensor device was assembled on fabricated paper-based electrodes composed by a carbon-ink as the counter and working (5 mm diameter) electrodes and, silver-ink as pseudo-reference electrode (Fig. 1). Detailed description of the procedure of fabrication of these electrodes was described elsewhere [9]. The electrochemical measurements were carried out with a potentiostat/galvanostat from *Metrohm Autolab* and a PGSTAT302N with an FRA module, through an interface switch box from *BioTid Eletrónica*, and controlled by ANOVA software. All the presented potential values are against the silver pseudo-reference.

Raman spectroscopy was performed by using a Thermo Scientific DXR Raman microscope system with a 785 nm excitation laser, combined with a 50× objective magnification. Raman spectra were collected with an incident maximum laser power of 3 mW and through a slit aperture of 50 μm. Photobleaching was set to 20 min. For Raman measurements, data analysis was performed with OMNIC software.

Scanning Electron Microscopy (SEM) analysis was performed in order to evaluate the morphology of the polymeric films modified on

Table 1
Comparison of the different sensors for 3-nitrotyrosine detection in biological matrices.

Method	Substrate	Linear range	LOD	Sample	Ref.
Electrochemical detection + MIP	Bimetallic Fe/Pd nanoparticles	21.6–3833 nM	5.3 nM	Human blood Urine	[30]
Electrochemical detection + MIP	GCE electrode with AuNPs	0.2–50.0 μM	50.0 nM	Human serum Urine	[31]
Fluorescent detection + MIP	Carbon dots	0.050–1.85 μM	17 nM	Human serum	[31]
HPLC detection with SPE + MIP	—	11.1–243 nM	3.1 nM	Human urine	[32]
SPR detection	Graphene	2.21–4421 pM	0.57 pM	Human serum	[33]

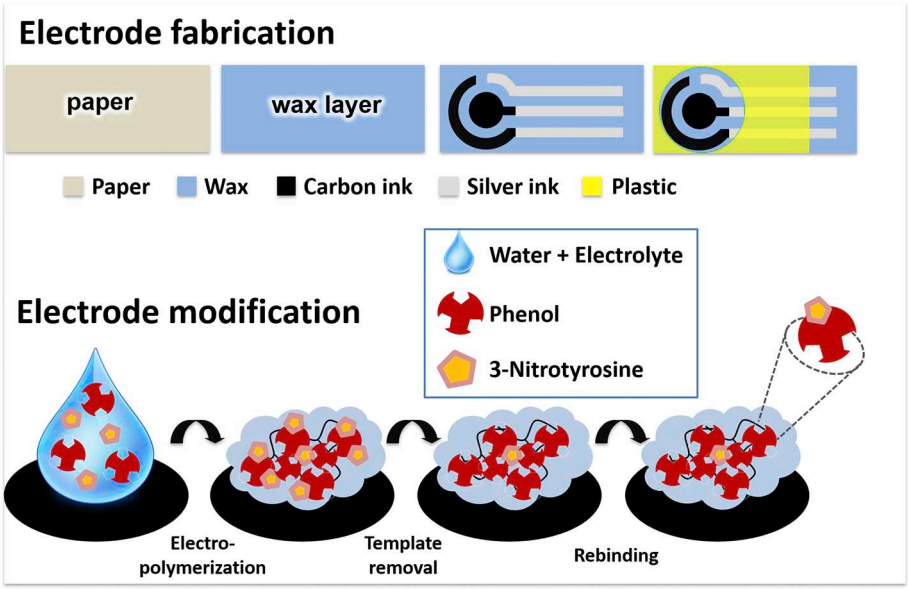

Fig. 1. Illustration of the sensor film fabrication by molecular imprinting for recognition of 3-nitrotyrosine.

the electrode surface, by using a Carl Zeiss AURIGA Crossbeam SEM-FIB workstation, operating with a voltage of 5 kV.

2.3. Electrochemical assay

Initially, the carbon surface of the electrodes was electrochemically cleaned by performing voltammetric sweeps between −0.2 V and + 1.5 V in PBS at pH 7.4, until a stable voltammogram was obtained (more or less 100 cycles). Before use, sensors were well dried with nitrogen and stored at room temperature.

Cyclic voltammetry (CV) assays were performed at different potential windows in order to evaluate the electroactive behaviour of the compounds. Each modification performed on the paper-based electrodes was electrochemically characterized by electrochemical impedance spectroscopy (EIS) of a 5 mM solution of $K_3[Fe(CN)_6]$ and $K_4[Fe(CN)_6]$, prepared in phosphate buffer solution (0.1 M, pH 6.0). EIS experiments were carried out over the frequency range 0.01 Hz to 100 kHz. All measurements were performed by covering the three electrodes of the paper-based sensor with a volume solution of 200 µl.

The detection of 3-NT molecule was followed by means of differential pulse voltammetry (DPV) in the potential range 0 V to +0.4 V, at a scan-rate 25 mV/s, pulse amplitude 25 mV and pulse width 50 ms. Before DPV measurement, the analyte was pre-concentrated at the electrode surface by applying a potential value of −1 V, for an optimized time of 60 s. All experiments were conducted in triplicate at room temperature. Calibration curves were made with fresh 3-NT standard solutions ranging from 100 nM to 1 mM.

2.4. Assembly of the imprinted-based (bio)sensor

The molecularly-imprinted polymer (MIP) film was deposited on the surface of the carbon-coated electrode through bulk polymerization. Initially, the electrodes were subjected to 5 voltammetric scans over the potential range − 0.2 V to +1.5 V in H_2SO_4 0.5 M solution, as an electrochemical cleaning procedure. Afterwards, the electropolymerization was performed by applying cyclic voltammetry sweeps ranging between +0.2 V and + 0.8 V, at a scan-rate of 50 mV/s, in KCl solution (0.1 M, pH 5.9) containing both phenol monomer and the template molecule 3-NT. Then, the template removal was made by incubation of the working electrode in a methanol:water solution (1:10, *v/v*) for 2 h, at room temperature, followed by 1 h stabilization in phosphate buffer solution. These solutions were prepared daily and all experiments were carried out at room temperature. Moreover, excluding the presence of 3-NT molecule, a similar procedure was taken in the fabrication of blank control material, named non-imprinted polymer-modified electrodes (NIP).

2.5. Analysis of urine samples

The selectivity features of the MIP-based sensor were directly assessed in human urine samples, due to their complex matrix. The urine samples were collected in sterile falcon tubes to avoid contamination and, afterwards, the fresh urine samples were frozen and stored in aliquots of 1 ml. Before the analysis, the samples were diluted in phosphate buffer solution (0.1 M, pH 6.0) in a 1:10 ratio. The detection of 3-NT in urine samples was performed by immersing the MIP-based device in the diluted samples, followed by a negative potential accumulation and finally DPV analysis. The same procedure was taken to the NIP control electrode.

3. Results and discussion

3.1. Electrochemical study

In the last years, the study of electrochemical oxidation of organic substances has been employed as a promising technique for analytical purposes. Herein, in order to evaluate the electrochemical behaviour of 3-nitrotyrosine (3-NT) in PBS solution (10 mM, pH 7.4), cyclic voltammetric sweeps were scanned in different directions over the potential range − 1.0 V and + 1.0 V, at a scan-rate of 50 mV/s. As depicted in Fig. 2A, two well-defined oxidation peaks were observed at +0.20 V and + 0.93 V, and a reduction peak around −0.85 V. This outcome is in accordance with our previous electrochemical study performed with the same modified-electrodes [9] and interestingly, we have found that the first anodic peak at +0.20 V depended of the occurrence of the cathodic peak. Hence, the results obtained by CV seemed to indicate that the earlier oxidation reaction corresponded to sub-species generated at the carbon surface after the reduction of 3-NT occurred at −0.85 V. Although there are already some electrochemical sensor devices based on the electro-oxidation of 3-NT for detection applications [29,30], to the best of our knowledge, this is the first time that this low oxidation peak potential (+0.20 V) has been chosen to follow this target molecule. The main advantages of working with this narrow potential window are that the oxidation reaction occurring on

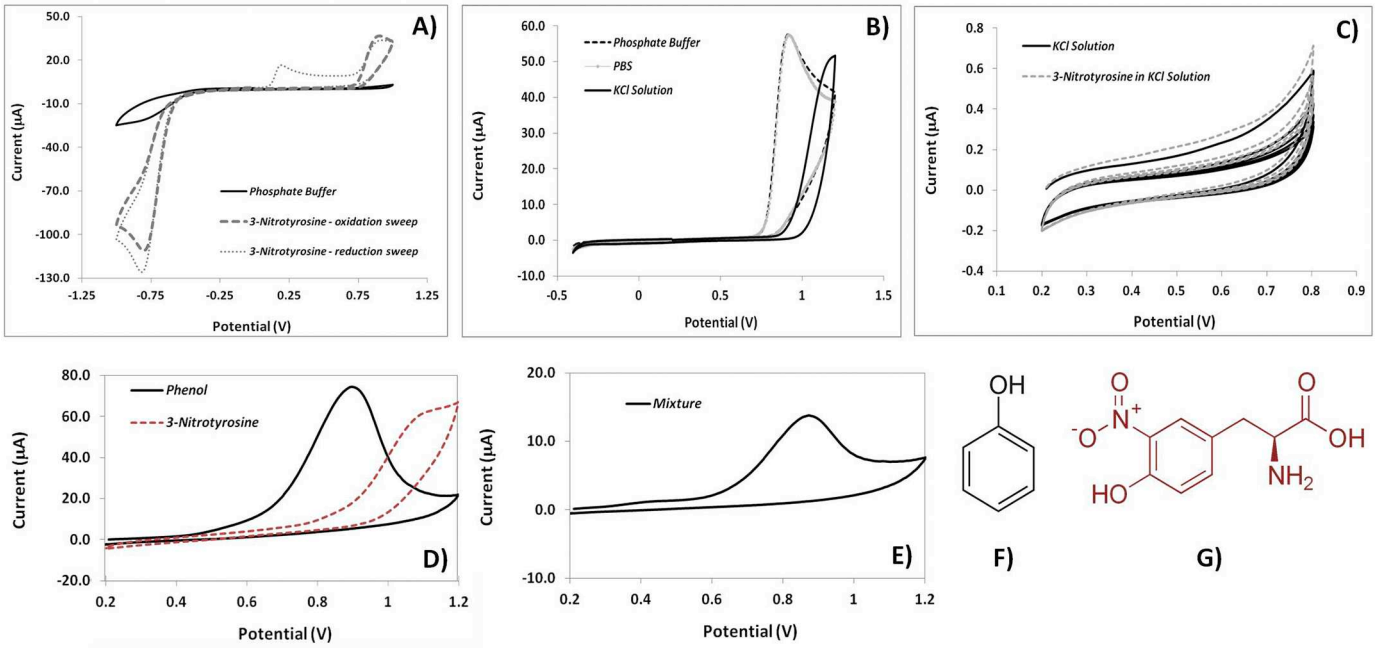

Fig. 2. Cyclic voltammograms of 3-nitrotyrosine in A) PBS solution, at different scan directions, over the potential range − 1 V to +1 V; B) three different electrolyte solutions, over the potential range − 0.4 V to +1.2 V; and C) KCl solution, over the potential range + 0.2 V to +0.8 V. Cyclic voltammograms of D) phenol and 3-nitrotyrosine, individually and E) mixture phenol +3-nitrotyrosine. Chemical representation of F) phenol and G) 3-nitrotyrosine.

the surface of the modified electrode is more favourable; there is no need to apply high voltage to the electrode system that can cause an overcharge and, consequently, could compromise the performance of the silver pseudo-reference; and also, it allows to eliminate the interference of other electroactive species found in biological matrices (uric acid, ascorbic acid, etc), which occurs at higher potential values [34–36].

The effect of different buffer and electrolyte species on the oxidation peak potential was also assessed by CV in a solution containing 4 mM of 3-NT (Fig. 2B). For this study, we have tested phosphate buffer solution (0.2 M, pH 7.0), PBS solution (10 mM, pH 7.4) and KCl solution (0.1 M, pH 5.9). Despite the difference on the salt species and concentration, it could be noticed that PBS and phosphate buffer solutions exhibited similar current and potential values, while in KCl solution we could observe that the oxidation peak potential of 3-NT shifted to a more positive position. This last result can be advantageous in order to guarantee a wider potential window in which 3-NT molecule does not display electroactive properties. Furthermore, Fig. 2C shows cyclic voltammograms in KCl solution alone and 3-NT in KCl solution, confirming that in the potential range + 0.2 V to +0.8 V there is no evidence of oxidation reaction of 3-NT.

Under the scope of this work, phenol has been chosen as the structural monomer to grow the imprinted polymeric matrix. It is a non-conducting material, holding good stability properties and typically known electro-oxidation properties. Several mechanisms regarding the oxidation of phenol and phenol derivatives have been described on gold [37] and platinum [38,39] surfaces, but less on glassy carbon electrodes [40,41]. Among others, experimental parameters, such as, temperature, concentration of the monomer, electrolyte type and pH of the applied electrolyte have proven to influence the electrochemical oxidation of phenol [38,39].

Fig. 2D displays cyclic voltammograms scanned over the potential range + 0.2 V to +1.2 V, at a scan-rate of 50 mV/s, for a 10 mM solution of phenol and a 4 mM solution of 3-NT, individually, both prepared in KCl 0.1 M solution (pH 5.9). As expected, these results indicated an irreversible oxidation reaction of the phenol monomer occurring on the electrode surface, around +0.9 V. Furthermore, in accordance with our previous data, 3-NT alone exhibited an anodic peak at higher potential values. Meanwhile, Fig. 2E showed the voltammetric sweep performed on the mixture phenol and 3-NT in KCl 0.1 M solution and only one well-defined oxidation peak was observed, meaning that under this experimental conditions it was not possible to separate accurately phenol (Fig. 2F) and 3-NT (Fig. 2G) electro-oxidations. In sum, the electropolymerization of phenol was carried out herein over the potential range + 0.2 V to +0.8 V, in order to avoid any kind of oxidation reaction that could modify or entrap irreversible 3-NT molecule in the polymeric matrix.

3.2. Electropolymerization of phenol - MIP versus NIP

Herein, electropolymerization was the approach chosen to assemble the biomimetic material because we can precisely tune the thickness and growth of the film in-situ, without using additional initiator species. Briefly, electro-oxidation of phenol occurs through the formation of the phenoxy radical, that can react with other species present in the solution generating products or else reacts with other phenol molecules producing a dimeric radical. Usually, the rate-determining step for phenolic compounds is one electron reaction, such as phenoxy radical forming [35]. The polymerization curves corresponding to the molecular (MIP) and non-molecular (NIP) imprint polymers for the 1st and 5th scan cycles are shown in Fig. 3A and B, respectively. As expected, voltammograms displayed an irreversible oxidation reaction of the monomer for both NIP and MIP materials, with NIP holding a higher current peak. It was also observed that the potential of the oxidation peak did not suffer any change with the increasing of the number of cycles. This behaviour was attributed to the electrode fouling produced by the formation of a non-conductive polymeric layer resulting from phenol oxidation that blocks the electrode surface. Moreover, the current peaks gradually decreased with the number of cycles, which is another characteristic assigned to the growth of non-conducting polymers [37]. In addition, no significant difference was observed in the cyclic voltammograms with and without the template molecule, shown in Fig. 3B, by the similar amplitude current obtained in the end of the polymerization reaction.

One of the great advantages of using an electropolymerization approach is their ability to finely tune the amount of deposited polymer,

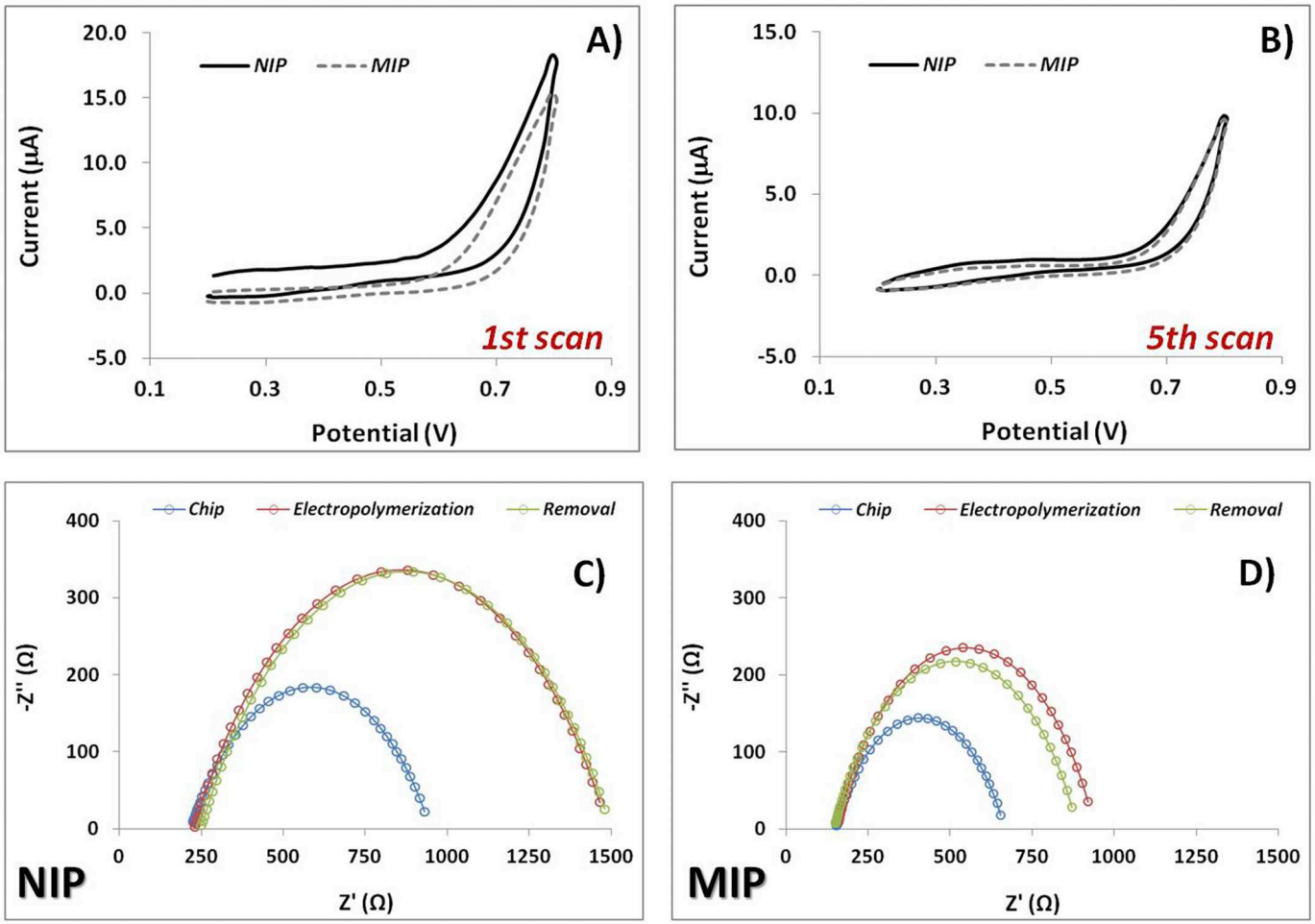

Fig. 3. Cyclic voltammograms of NIP and MIP electrodes during electrochemical polymerization of phenol for the A) 1st and B) 5th scan cycle, in KCl solution (0.1 M, pH 5.9). EIS obtained for each step of the construction for C) NIP and D) MIP electrodes, in 5 mM solution of $K_3[Fe(CN)_6]$ and $K_4[Fe(CN)_6]$ prepared in phosphate buffer solution (0.1 M, pH 6.0).

by adjusting the duration of the applied voltage (number of cycles), the scan-rate and the potential window. The thickness (*d*) of the polymer film can be roughly estimated from the charge (*Q*) passed during electropolymerization, according to Faradays law [37]. By applying the following relation:

$$d = QM/FA\rho$$

where *M* is the molar mass of the monomer, *F* is the Faraday constant (96,485C/m^2), ρ is the density of the polymer, taken to be 1 g/cm^3 for polyphenols and *A* is the electrode surface geometric area. Herein, the thickness of the polymeric film was about ~2.5 nm. One of the limitations of using non-conducting polymers, such as phenol and phenol derivatives, is because of their self-limited growth on the electrode surface and, therefore, resulting in very thin films (< 100 nm) [38]. Here, the target molecule to be imprinted is quite small and, consequently, there is no need to assemble thicker films. Moreover, previous electrochemical studies have used imprinted electrodes, modified with non-conducting films, holding ultrathin polymeric layers in order to improve the sensitivity of the device [39].

Nowadays, impedance techniques are being widely applied to monitor variations in electrical properties as a direct response of the bio-recognition events that take place at the surface of the electrodes. Moreover, EIS holds the advantage of not causing any damage to the analysed surface and do not introduce any disturbance in the studied system. Herein, along the fabrication of MIP and NIP, the electrodes were stepwise characterized by means of EIS, using as redox probe a 5 mM solution of $K_3[Fe(CN)_6]$ and $K_4[Fe(CN)_6]$ prepared in 0.1 M phosphate buffer. Usually, the impedance spectrum includes a semi-circular portion at higher frequencies and a linear portion at lower frequencies which corresponds to the electron-transfer resistance (*Rct*) and the diffusion process, respectively. Fig. 3 also displays the Nyquist plots showing each step of the modification of the fabricated NIP (Fig. 3C) and MIP (Fig. 3D) electrodes. As expected, the electropolymerization of phenol resulted in a substantial increase of the Rct value due to the blocking of electron transfer by the polymeric matrix. Moreover, the results obtained for NIP and MIP after electropolymerization suggested that the non-imprinted coated electrode exhibited stronger insulating properties, which constitutes an evidence of the presence of the template molecule on the imprinted material, which partially hinders the growth of polyphenol film. Afterwards, the removal step caused a small decrease of the Rct value only on the MIP modified electrode, suggesting that the formation of the imprinted cavities occurred and, consequently, electronic diffusion was facilitated. In the literature, there are different approaches to extract a template molecule from the polymeric matrix of MIP-based sensing devices, including washing with sulphuric acid, acetic acid, methanol, ethanol, etc. Furthermore, previous works have already been well succeeded in the removal of template protein by using mixed organic solvents, such as, PBS:methanol (10:1, *v/v*), without causing degradation of the polyphenol film [37] or even incubation in ethanol:water (5:1, *v/v*) mixture [40]. In the current study, a mixture methanol:water (1:10, *v/v*) was chosen as the mix solvent with more satisfactory results,

because it was able to efficiently extract the 3-NT template without causing any degradation or modification to the polymeric material.

3.3. Optimization of experimental conditions during MIP assembly

3.3.1. Effect of scan-rate and number of electropolymerization cycles

Beside thickness, the density of polyphenol films can also be adjusted by controlling some variables during electropolymerization, such as, the rate of film growth and the number of voltammetric sweeps. Hence, comparative studies were performed by using EIS to characterize the charge transfer properties of different modified electrodes, at various experimental conditions.

Herein, the MIP-based electrodes were assembled with three different scan-rate values, as shown in the Nyquist plots of Figs. S1A–C. Firstly, the only MIP-coated material that presented a decrease of the Rct value as the result of the creation of imprinted cavities was the one assembled at a scan-rate of 50 mV/s, while the others suffered an increasing variation. Moreover, the electropolymerization performed at 50 mV/s scan-rate was responsible for the formation of a less insulating surface (366 Ω), which could be an advantage for the successful extraction of the template molecule from the MIP matrix [38]. In addition, Fig. S1D–F illustrate the Nyquist diagrams obtained during the fabrication of the MIP electrodes using 2, 5 and 10 CV cycles, respectively. Generally, the detection capability of a sensor is highly affected by the number of scanning cycles used in the formation of the polymeric material. For instance, a lower number of cycles is often associated to a favourable analytical performance whereas a higher number of voltammetric cycles can led to the formation of a thicker film with less accessible imprinted sites and, consequently, less sensitivity [40,41]. Furthermore, a high number of scanning cycles increased the possibility of 3-NT template molecules becoming trapped in the polymer matrix. Herein, our data showed that the higher % of template removal was obtained for the MIP prepared with 5 scanning cycles (~10%), when compared with 2 cycles (~4%) and 10 cycles (~3%). Therefore, 5 cycles with a scan-rate of 50 mV/s were selected for the growth of the non-conductive polymer layer.

3.3.2. Effect of monomer concentration

Among others already mentioned, polyphenol films hold a great advantage as a biomimetic matrix because it can be easily synthetized by electropolymerization from aqueous solutions of the monomer. In addition, the thickness of the imprinted layer can also be adjusted by optimization of the monomer concentration. Herein, EIS was used to follow the construction of NIP and MIP sensors, with two distinct concentrations of phenol: 1.0 mM (Fig. S2A) and 0.25 mM (Fig. S2B). As expected, the Rct values of both NIP and MIP are shifted towards higher values for increasing phenol bulk concentration. It was interesting to observe that the stronger insulating character of the non-imprinted coated electrode compared to the imprinted-device was maintained in both concentrations. The obtained data also have showed that in the case of 1 mM of phenol (Fig. S2A) the films formed were quite resistive (4 kΩ < Rct < 7 kΩ), which may be a limitation in terms of sensor sensitivity.

In addition, the rebinding of 3-NT molecule was quantified by means of differential pulse voltammetry (DPV). In practice, the current data accounted the occupation of the imprinted cavities in the MIP electrode by the template molecules, followed by their electro-oxidation. Fig. S2C presents DPV calibration curves plotted with the logarithm of current of MIP sensors against the logarithm concentration of 3-NT. The comparison of the two curves have showed that a lower concentration of phenol (0.25 mM) enabled lower detection limits when compared to 1 mM concentration of phenol, which is in agreement with our previous conclusions that thicker films hold less number of imprinted cavities and, consequently, less sensitive responses. So, a concentration of phenol monomer of 0.25 mM was chosen for further studies.

3.3.3. Effect of imprinted 3-NT concentration

The concentration of the template was another crucial parameter that could influence the MIP performance. Specifically, the ratio template-monomer of MIP determines the number of binding sites available for the selective rebinding of the molecules and, consequently, the detection limit of the (bio)sensor. In parallel, the interaction of these molecules with the phenol units during the assembly of the polymeric matrix also dictates the formation of stable and specific binding cavities. Phenol-based MIP films have been widely applied as recognition matrices in (bio)sensors due to their ability to interact with other molecules through the existence of the π donor-acceptor interactions [39].

Herein, the effect of 3 different concentrations of 3-NT was investigated during phenol electropolymerization. Fig. S3A illustrates the charge variation that MIP electrodes suffer during the 5 scanning cycles and Fig. S3B displays the corresponding Nyquist diagrams obtained after the electropolymerization step. Data showed that for increasing concentrations of 3-NT the tendency was to obtain a less insulating polymeric layer, which is in agreement with our previous results, where the presence of the template molecule can partially hinder the growth of polyphenol film. Afterwards, the rebinding of 3-NT molecule was also investigated by means of DPV for the 3 different concentrations, 0.05 mM (Fig. S3C), 0.25 mM (Fig. S3D) and 0.50 mM (Fig. S3E). Overall, the higher concentration of imprinted molecule (0.50 mM) enabled the detection of lower concentrations in comparison with the other imprinted concentrations of 3-NT, which constitutes a strong indication that using higher concentration of template molecule results in the creation of more imprinting sites available for the rebinding (see Fig. S3F).

Although not presented here, along this optimization study the experimental conditions of the DPV measurements where finely tuned in order to get the higher response current. Specifically, one of the great advantages of our approach was the elimination of long incubation periods, by applying a pre-accumulation potential before each electrical measurement, in order to attract the target molecule to the region near the electrode surface. In addition, this pre-concentration step of 3-NT on the sensor surface before each DPV measurement is also necessary to promote the reduction of the species that will be afterwards oxidize at +0.20 V.

In all experiments, the accumulation potential value used before the DPV measurement was −1 V and different accumulation times were tested, namely 30, 60 and 180 s. Our best electrochemical response was obtained for 60 s of accumulation at −1 V and so, these conditions were applied along this work.

3.4. Characterization of the modified paper-electrodes

Raman spectroscopy has been widely used as a popular tool for the characterization and structural organization of carbon materials. Herein, Fig. 4A presented the Raman spectra for the different modifications performed on the paper-based electrodes. Firstly, all samples presented two well distinct peaks occurring typically in graphite-based substrates, the so-called G and D peaks, lying at around 1570 and 1310 cm^1, respectively. In the clean carbon-coated electrode, the G band appeared at 1584 cm^{-1} and was assigned to the C/C stretching in graphitic materials, composed of sp^2 bonded carbon in planar sheets [42]; the D band appeared around 1307 cm^{-1} and is often referred to as the disorder band or the defect band. In order to characterize the level of disorder within the carbon material, the intensity peak ratio between the D and G bands (I_D/I_G) was analysed.

Table 2 displays the peak positions of the G and D bands in the materials that were investigated, as well as the corresponding intensities. Although the I_D/I_G ratios showed a similar tendency among the different electrodes, it was interesting to observe that the introduction of the polymeric material, on both NIP and MIP cases, resulted in a carbon system with less level of disorder. Moreover, another typical Raman band of carbon related materials is the 2D band, usually

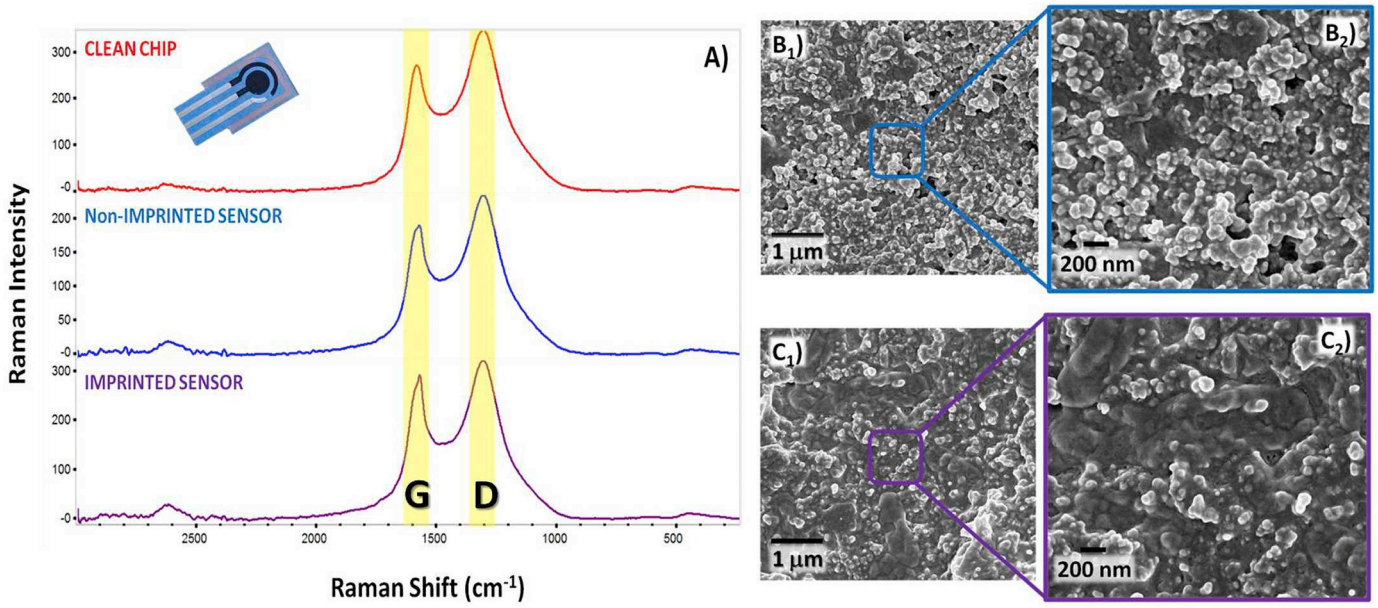

Fig. 4. A) Raman spectra of clean carbon-based electrode, NIP and MIP-modified surfaces. SEM images of B) NIP and C) MIP materials.

Table 2
Analytical data obtained from the Raman spectra related to the different modifications.

Sample	*D* Position (cm^{-1})	Intensity	*G* Position (cm^{-1})	Intensity	I_D/I_G
Clean chip	1307.21	347.10	1584.77	269.56	1.29
NIP	1308.13	233.63	1574.36	188.59	1.24
MIP	1310.11	320.74	1572.68	290.53	1.10

located around 2700 cm^{-1}. As can be seen on Fig. 4A, this band is almost absent in the spectrum of the clean carbon-coated chip, but on both NIP and MIP materials this signal appears enhanced, which constitutes another strong evidence of the deposition of the polymeric material.

Surface morphology of the prepared NIP and MIP electrodes was further studied by means of SEM, as can be seen in Fig. 4B and C, respectively. The main difference observed between both materials was that the NIP surface presented a higher distribution of small islets while in the MIP surface the growth of the polymeric film seemed more even and well spread on the electrode. Moreover, the globular structure obtained for the phenol polymeric film was in agreement with a previous study, performed in a different substrate material [12]. Although it was not possible to visualize the imprinted cavities, due to the small dimensions of 3-NT molecule, the differences observed in the SEM images can be an indication of the presence of 3-NT molecule during electropolymerization that resulted in a different structural polymeric growth.

3.5. Performance of the imprinted-sensor

3.5.1. Calibration curve

The main analytical features of the 3-NT (bio)sensor were evaluated by DPV calibration curves, carried out under the optimal experimental conditions (potential range 0 V to +0.4 V, at a scan-rate 25 mV/s, pulse amplitude 25 mV and pulse width 50 ms with a pre-accumulation step at −1 V for 60 s). Fig. 5A and B shows the calibration curves plotted with the logarithm concentration of 3-NT versus the logarithm of current for MIP and NIP sensors, respectively. As can be seen, a linear tendency was obtained for both imprinted and non-imprinted materials from 500 nM to 1000 µM, but the MIP sensor showed higher sensitivity (*slope = 0.7591 ± 0.0613, abscissa = −1.154 ± 0.468*), better linearity (r^2 = *0.9943*) and better reproducibility (smaller error-bars) in comparison with the NIP (*slope = 0.5941 ± 0.1886, abscissa = −0.903 ± 0.700*). The limit of detection (*LOD*) was 22.3 nM, calculated as three times the standard deviation from the blank measurement (in the absence of template molecule). The inset graphic representation illustrated in Fig. 5A concerns the DPV data obtained for the MIP-based sensor for the respective concentrations of 3-NT molecule. The precision of both modified-electrodes, for 3 different independent experiments, is also presented on Fig. 5, over the entire concentration range.

Compared with other methods (*see* Table 1), the *LOD* found here is in agreement with the works reported in literature involving a molecular imprinting technology coupled with electrochemical sensing. Interestingly, when reviewing the construction of these imprinted-based sensors, it was generally found that the use of amplification steps, such as, the incorporation of nanomaterials, was required to achieve such low detection limits. Besides, another relevant advantage of our electrochemical device is the use of a label-free approach that enables decreasing substantially the analysis time and, consequently, becoming more affordable. The use of a paper support is also a great advantage in terms of cost.

3.5.2. Urine samples

In order to evaluate the applicability of the proposed MIP-modified electrode in real samples, the electrochemical readings of 3-NT standards were performed in a background of human urine samples. Thus, diluted blank urine samples (1:10 in phosphate buffer) were spiked with different concentrations of 3-NT and analysed by means of DPV measurements. As can be seen in Fig. 6A, the MIP material enabled the quantification of 3-NT from 5 µm to 1 mM, with relative standard deviations (RSD) ranging 1 to 2%. In contrast, the NIP material (Fig. 6B) showed a non-reproducible response along a narrow range of concentrations, which could be a strong indication of the non-specific adsorption phenomena occurring at the surface of the polymeric material.

Overall, these results demonstrated the capability of this imprinted-modified sensor assembled on paper support to sensitively quantify 3-NT in urine samples. Despite the existence of few sensor devices with similar *LODs* for the detection of 3-NT, our purpose herein was the development of a quick, facile, reproducible and low-cost paper-based (bio)sensor suitable to be applied as a portable tool in *POC* screening. Besides the lower LOD, the introduction of a molecularly imprinted

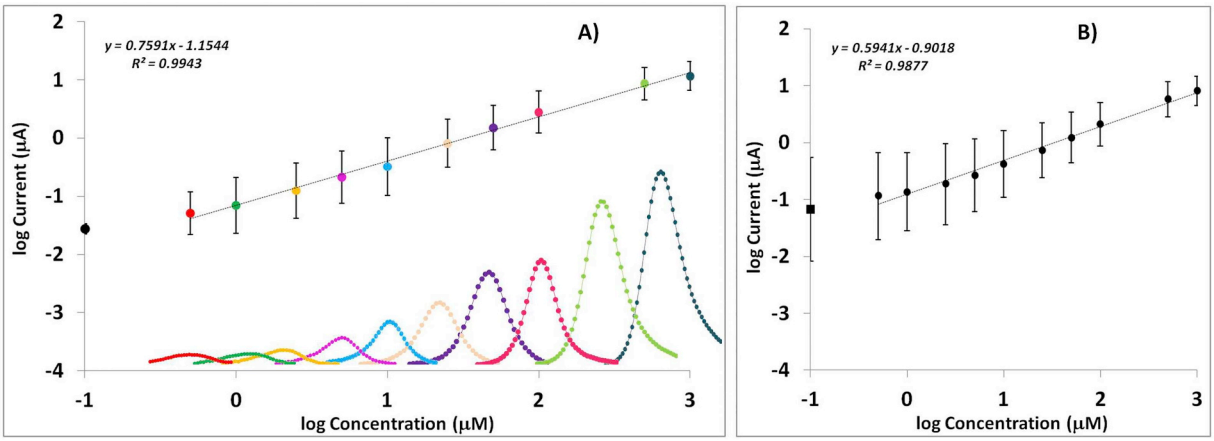

Fig. 5. Calibration curves corresponding to the response of A) MIP and B) NIP sensors against the concentration of 3-nitrotyrosine. The inset figure is related to the DPV recordings for each standard concentration.

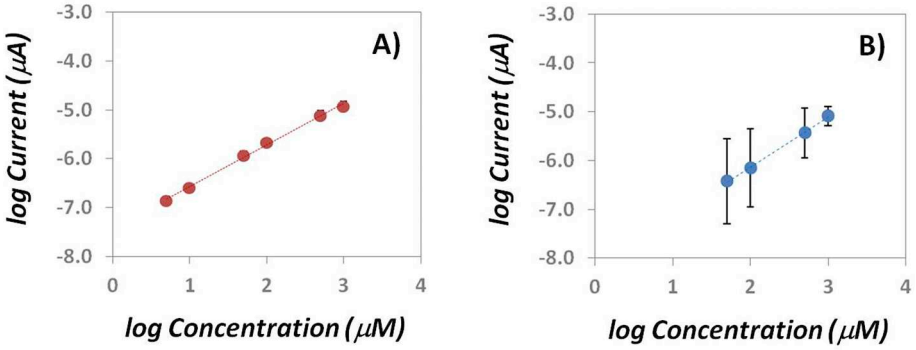

Fig. 6. Calibration curves corresponding to the response of A) MIP and B) NIP sensors against the concentration of 3-nitrotyrosine, performed in 1:10 diluted human urine samples.

coating enabled our paper-based electrochemical platform with good selectivity performance. Comparing this work to our previous work [9] in terms of analytical performance, it was clear that the MIP was responsible for the high selectivity to the electrochemical signal, which in turn enabled the analysis of complex samples (something not tested before).

4. Conclusions

This study reports a label-free electrochemical (bio)sensor platform for in-situ detection of 3-NT. Herein, the application of an imprinted material could enable specific rebinding of molecules into the imprinted cavities of MIP-modified films, improving selectivity features of the (bio)sensor device. The optimization of some experimental parameters during electropolymerization, such as, scan-rate, number of cycles, monomer and template concentration, among others, allowed to finely tune the thickness and growth of the polymeric matrix.

The imprinted-based sensor showed high electrochemical performance on the oxidation of 3-NT biomarker over the concentration range 500 nM to 1 mM and a low detection limit (22.3 nM). Selectivity towards 3-NT over a wide range of concentrations was also successfully obtained with the analysis of urine samples. Although the obtained LOD was not the lower value found in the literature, the electrochemical performance of this paper-based (bio)sensor greatly satisfies the requirements of a selective, reproducible, disposable and sustainable sensing platform. Overall, the main advantage of this (bio)sensor device in comparison with other existing sensors is its potential to be easily and costly miniaturized in the future.

CRediT authorship contribution statement

Gabriela V. Martins: Investigation, Methodology, Validation, Visualization, Formal analysis, Data curation, Writing - original draft.**Ana C. Marques:**Resources, Methodology, Data curation, Writing - review & editing.**Elvira Fortunato:**Conceptualization, Funding acquisition, Supervision, Writing - review & editing.**M. Goreti F. Sales:**Conceptualization, Supervision, Funding acquisition, Project administration, Writing - review & editing.

Declaration of competing interest

The author(s) declare no competing financial interests.

Acknowledgments

Fundação para a Ciência e Tecnologia (FCT) supported this work through FEDER funds from COMPETE 2020 Program and National Funds, under the project PTDC/AAG-TEC/5400/2014 & POCI-01-0145-FEDER-016637, NORTE-01-0145-FEDER-024358, UID/CTM/50025/2019 and the PhD Grants references SFRH/BD/94159/2013 (GVM) and SFRH/BD/115173/2016 (ACM). H2020 also supported this work through the project MindGAP/FET-Open/GA829040.

Appendix A. Supplementary data

Supplementary data to this article can be found online at https://doi.org/10.1016/j.sbsr.2020.100333.

References

[1] J. Muñoz, R. Montes, M. Baeza, Trends in electrochemical impedance spectroscopy involving nanocomposite transducers: characterization, architecture surface and bio-sensing, Trends Anal. Chem. 97 (2017) 201–215.

[2] K.K. Mistry, T. Sagarika Deepthy, C.R. Chaudhuri, H. Saha, Electrochemical characterization of some commercial screen-printed electrodes in different redox substrates, Curr. Sci. 109 (2015) 1427–1436.

[3] G. Ibáñez-Redín, R.H.M. Furuta, D. Wilson, F.M. Shimizu, E.M. Materon, L.M.R.B. Arantes, et al., Screen-printed interdigitated electrodes modified with nanostructured carbon nano-onion films for detecting the cancer biomarker CA19-9, Mater. Sci. Eng. C 99 (2019) 1502–1508.

[4] C. Parolo, M. Medina-Sánchez, H. Montõn, A. De La Escosura-Muñiz, A. Merkoçi, Paper-based electrodes for nanoparticles detection, Part. Part. Syst. Charact. 30 (2013) 662–666.

[5] N. Sharma, T. Barstis, B. Giri, Advances in paper-analytical methods for pharmaceutical analysis, Eur. J. Pharm. Sci. 111 (2018) 46–56.

[6] M. Hasanzadeh, N. Shadjou, Electrochemical and photoelectrochemical nano-immunesensing using origami paper based method, Mater. Sci. Eng. C 61 (2016) 979–1001.

[7] Q.X. Wang, S.F. Xue, Z.H. Chen, S.H. Ma, S. Zhang, G. Shi, et al., Dual lanthanide-doped complexes: the development of a time-resolved ratiometric fluorescent probe for anthrax biomarker and a paper-based visual sensor, Biosens. Bioelectron. 94 (2017) 388–393.

[8] Q.-M. Feng, J.-B. Pan, H.-R. Zhang, J.-J. Xu, H.-Y. Chen, Disposable paper-based bipolar electrode for sensitive electrochemiluminescence detection of a cancer biomarker, Chem. Commun. (Camb.) 50 (2014) 2–4.

[9] G.V. Martins, A.C. Marques, E. Fortunato, M.G.F. Sales, Novel wax-printed paper-based device for a direct electrochemical detection of 3-nitrotyrosine biomarker, Electrochim. Acta 284 (2018) 60–68.

[10] K. Kotova, M. Hussain, G. Mustafa, P.a. Lieberzeit, MIP sensors on the way to biotech applications: targeting selectivity, Sensors Actuators B Chem. 189 (2013) 199–202.

[11] S. Mamo, J. Gonzalez-Rodriguez, Development of a molecularly imprinted polymer-based sensor for the electrochemical determination of Triacetone Triperoxide (TATP), Sensors. 14 (2014) 23269–23282.

[12] G.V. Martins, A.C. Marques, E. Fortunato, M.G.F. Sales, 8-hydroxy-2′-deoxyguanosine (8-OHdG) biomarker detection down to picoMolar level on a plastic antibody film, Biosens. Bioelectron. 86 (2016) 225–234.

[13] L.K. Singh, M. Singh, M. Singh, Biopolymeric receptor for peptide recognition by molecular imprinting approach-synthesis, characterization and application, Mater. Sci. Eng. C 45 (2014) 383–394.

[14] P.S. Sharma, A. Pietrzyk-Le, F. D'Souza, W. Kutner, Electrochemically synthesized polymers in molecular imprinting for chemical sensing, Anal. Bioanal. Chem. 402 (2012) 3177–3204.

[15] P. Wang, G. Sun, L. Ge, S. Ge, J. Yu, M. Yan, Photoelectrochemical lab-on-paper device based on molecularly imprinted polymer and porous Au-paper electrode, Analyst. 138 (2013) 4802–4811.

[16] G. Sun, P. Wang, S. Ge, L. Ge, J. Yu, M. Yan, Photoelectrochemical sensor for pentachlorophenol on microfluidic paper-based analytical device based on the molecular imprinting technique, Biosens. Bioelectron. 56 (2014) 97–103.

[17] M.D. Evans, M. Dizdaroglu, M.S. Cooke, Oxidative DNA damage and disease: induction, repair and significance, Mutat. Res. 567 (2004) 1–61.

[18] S. Reuter, S.C. Gupta, M.M. Chaturvedi, B.B. Aggarwal, Oxidative stress, inflammation, and cancer: how are they linked? Free Radic. Biol. Med. 49 (2010) 1603–1616.

[19] I. Dalle-Donne, R. Rossi, R. Colombo, D. Giustarini, A. Milzani, Biomarkers of oxidative damage in human disease, Clin. Chem. 52 (2006) 601–623.

[20] H. Ahsan, 3-Nitrotyrosine: a biomarker of nitrogen free radical species modified proteins in systemic autoimmunogenic conditions, Hum. Immunol. 74 (2013) 1392–1399.

[21] K. Syslová, A. Böhmová, M. Mikoška, M. Kuzma, D. Pelclová, P. Kačer, Multimarker screening of oxidative stress in aging, Oxidative Med. Cell. Longev. 2014 (2014) 1–14.

[22] H. Ryberg, K. Caidahl, Chromatographic and mass spectrometric methods for quantitative determination of 3-nitrotyrosine in biological samples and their application to human samples, J. Chromatogr. B Anal. Technol. Biomed. Life Sci. 851 (2007) 160–171.

[23] H. Yang, Y. Zhang, U. Pöschl, Quantification of nitrotyrosine in nitrated proteins, Anal. Bioanal. Chem. 397 (2010) 879–886.

[24] Y. Kamisaki, K. Wada, K. Nakamoto, Y. Kishimoto, M. Kitano, T. Itoh, Sensitive determination of nitrotyrosine in human plasma by isocratic high-performance liquid chromatography, J. Chromatogr. B Biomed. Appl. 685 (1996) 343–347.

[25] A. Conventz, A. Musiol, C. Brodowsky, A. Müller-Lux, P. Dewes, T. Kraus, et al., Simultaneous determination of 3-nitrotyrosine, tyrosine, hydroxyproline and proline in exhaled breath condensate by hydrophilic interaction liquid chromatography/electrospray ionization tandem mass spectrometry, J. Chromatogr. B Anal. Technol. Biomed. Life Sci. 860 (2007) 78–85.

[26] D. a Richards, M. a Silva, A.J. Devall, Electrochemical detection of free 3-nitrotyrosine: application to microdialysis studies, Anal. Biochem. 351 (2006) 77–83.

[27] M.T. Frost, B. Halliwell, K.P. Moore, Analysis of free and protein-bound nitrotyrosine in human plasma by a gas chromatography/mass spectrometry method that avoids nitration artifacts, Biochem. J. 345 (2000) 453–458.

[28] J. Jin, C. Wang, Y. Tao, Y. Tan, D. Yang, Y. Gu, et al., Determination of 3-nitrotyrosine in human urine samples by surface plasmon resonance immunoassay, Sensors Actuators B Chem. 153 (2011) 164–169.

[29] E. Roy, S. Patra, R. Madhuri, P.K. Sharma, Developing electrochemical sensor for point-of-care diagnostics of oxidative stress marker using imprinted bimetallic Fe/Pd nanoparticle, Talanta. 132 (2015) 406–415.

[30] S. Wang, G. Sun, Z. Chen, Y. Liang, Q. Zhou, Y. Pan, et al., Constructing a novel composite of molecularly imprinted polymer-coated AuNPs electrochemical sensor for the determination of 3-nitrotyrosine, Electrochim. Acta 259 (2018) 893–902.

[31] R. Jalili, M. Amjadi, Bio-inspired molecularly imprinted polymer–green emitting carbon dot composite for selective and sensitive detection of 3-nitrotyrosine as a biomarker, Sensors Actuators B Chem. 255 (2018) 1072–1078.

[32] L. Mergola, S. Scorrano, R. Del Sole, M.R. Lazzoi, G. Vasapollo, Developments in the synthesis of a water compatible molecularly imprinted polymer as artificial receptor for detection of 3-nitro-l-tyrosine in neurological diseases, Biosens. Bioelectron. 40 (2013) 336–341.

[33] S.P. Ng, G. Qiu, N. Ding, X. Lu, C.-M.L. Wu, Label-free detection of 3-nitro-l-tyrosine with nickel-doped graphene localized surface plasmon resonance biosensor, Biosens. Bioelectron. 89 (2016) 468–476.

[34] U. Chandra, Determination of dopamine in presence of uric acid at poly (eriochrome black t) film modified graphite pencil electrode, Am. J. Anal. Chem. 2 (2011) 262–269.

[35] L. Jia, H. Wang, Electrochemical reduction synthesis of graphene/Nafion nanocomposite film and its performance on the detection of 8-hydroxy-2′-deoxyguanosine in the presence of uric acid, J. Electroanal. Chem. 705 (2013) 37–43.

[36] A. Martín, P. Batalla, J. Hernández-Ferrer, M.T. Martínez, A. Escarpa, Graphene oxide nanoribbon-based sensors for the simultaneous bio-electrochemical enantiomeric resolution and analysis of amino acid biomarkers, Biosens. Bioelectron. 68 (2015) 163–167.

[37] T.L. Panasyuk, V.M. Mirsky, S.A. Piletsky, O.S. Wolfbeis, Electropolymerized molecularly imprinted polymers as receptor layers in capacitive chemical sensors, Anal. Chem. 71 (1999) 4609–4613.

[38] A.M. Spehar-Délèze, S. Anastasova, P. Vadgama, Electropolymerised phenolic films as internal barriers for oxidase enzyme biosensors, Electroanalysis. 26 (2014) 1335–1344.

[39] J.A. Ribeiro, C.M. Pereira, A.F. Silva, M.G.F. Sales, Electrochemical detection of cardiac biomarker myoglobin using polyphenol as imprinted polymer receptor, Anal. Chim. Acta 981 (2017) 41–52.

[40] G. Fang, G. Liu, Y. Yang, S. Wang, Quartz crystal microbalance sensor based on molecularly imprinted polymer membrane and three-dimensional Au nanoparticles@mesoporous carbon CMK-3 functional composite for ultrasensitive and specific determination of citrinin, Sensors Actuators B Chem. 230 (2016) 272–280.

[41] D. Duan, H. Yang, Y. Ding, D. Ye, L. Li, G. Ma, Three-dimensional molecularly imprinted electrochemical sensor based on Au NPs@Ti-based metal-organic frameworks for ultra-trace detection of bovine serum albumin, Electrochim. Acta 261 (2018) 160–166.

[42] L.G. Cançado, A. Jorio, E.H.M. Ferreira, F. Stavale, C.A. Achete, R.B. Capaz, et al., Quantifying defects in graphene via Raman spectroscopy at different excitation energies, Nano Lett. 11 (2011) 3190–3196.